DOE Award No. FG02-93ER14331

PI: Robert Bartynski
Rutgers University

Final Technical Report
31-March-2017

I. 1. Summary

During the term of this grant (02/15/11 to 02/14/16), we have been studying new aspects of the relationships between nanoscale surface features and heterogeneous catalysis or electrocatalysis. We concentrate on atomically rough and morphologically unstable surfaces of catalytic metal single crystals (Re, Ru, Ir) that undergo nanoscale faceting when interacting with strongly adsorbed species (e.g. O, N, C) at elevated temperatures.

The focus of our work is determining (a) the structure of the faceted metal surfaces, (b) the reactivity and selectivity of the planar and faceted metal surfaces in chemical and electrochemical reactions, and (c) use of faceted metal surfaces as nanotemplates for growth of metal nanoclusters and synthesis of metal monolayer electrocatalyst for hydrogen evolution reaction.

Our objectives are (a) to identify the causes of faceting and other nanoscale growth phenomena on faceted metal surfaces, and (b) to correlate surface structure and reactivity/ selectivity in heterogeneous catalysis and electrocatalysis with nanoscale features.

We have used multiple UHV surface science techniques for experimental measurements, which include AES, LEED, TPD, STM, LEIS, XPS, and electrochemical reactions, and DFT in combination with the *ab initio* atomistic thermodynamics approach for theoretical calculations.

We find that many planar metal surfaces that are rough on the atomic scale (e.g. fcc Ir(210), hcp Re($12\bar{3}1$), Re($11\bar{2}1$) and Ru($11\bar{2}1$)) are morphologically unstable and undergo faceting when interacting with strongly adsorbed species (e.g. O, N, C) at elevated temperatures. The faceted surfaces expose new crystal faces (facets) on the nanometer scale. We have used faceted surfaces as nanoscale model catalysts for chemical reactions and as nanotemplates for growth of nanoclusters and synthesis of nanoscale model electrocatalyst.

The main results since the last three-year report are (1) contributing an invited review paper to a book entitled "Catalysis by Materials with Well-Defined Structures" (Elsevier, B.V.), (2) discovering reversible transitions among various morphologies of the faceted Re($11\bar{2}1$) surface and identifying microscopic structural connections between the metastable facets that shed light on the mass transport pathways in the reversible morphological transitions of faceted Re($11\bar{2}1$), which is the first observation of reversible morphological transitions between different types of faceted metal single crystal surfaces, (3) discovering carbon-induced faceting of Re($11\bar{2}1$) and Re($12\bar{3}1$), which is the first real-space observation of C-induced faceting of metal surfaces, (4) finding nitrogen-induced reconstruction and faceting of Re($11\bar{2}1$) where the (2×1) reconstructed Re($11\bar{2}1$) surface acts as a precursor state for faceting of Re($11\bar{2}1$), (5) obtaining real-space images from oxygen-induced faceted Ru($11\bar{2}1$) and finding unique branching in oxygen-induced faceting of Ru($11\bar{2}1$), (6) determining the atomic geometries and energetics of adsorbates (N, C) on Re surfaces of planar ($11\bar{2}1$) and facets as well as constructing surface phase diagrams of C/Re and N/Re, (7) exploring reactivity and reaction pathway in oxidation of CO by NO on planar and faceted Ir(210), (8) characterizing adsorption sites of CO, O, NO, CO+O and CO+NO on planar and faceted Ir(210), (9) finding and elucidating the origin of structure sensitivity in adsorption and desorption of hydrogen on faceted Ir(210) versus planar Ir(210) by means of combined experiment

and calculation, (10) observing high reactivity of planar and faceted Ir(210) with 100% selectivity to N_2 in reduction of NO by acetylene at fractional acetylene pre-coverage as well as finding beneficial effects of sub-monolayer surface carbon on C-containing product selectivity, (11) discovering N_2O formation from ammonia oxidation by pre-adsorbed oxygen on planar and faceted Ir(210) as well as finding that product selectivity to N_2, N_2O or NO in the oxidation of ammonia by pre-adsorbed oxygen on Ir can be tuned by oxygen pre-coverage, surface structure, and facet size, which is the first observation of N_2O formation in catalytic ammonia oxidation under UHV conditions (1×10^{-9} Torr), (12) preferential nucleation and growth of gold nanoclusters on faceted O/Ru($11\bar{2}0$) with regular spacing and narrow size distribution, (13) synthesizing a nanoscale model electrocatalyst of Pt monolayer (ML) on faceted C/Re($11\bar{2}1$) that exhibits higher reactivity for hydrogen evolution reaction than Pt(111), which is the first application of faceted metal surfaces as nanotemplates for synthesis of nanoscale model electrocatalyst with well-defined (facet) structure and controlled (facet) size on the nanometer scale.

We have continued successful collaborations with theorists at Ulm University in Germany who have contributed substantially to our understanding of facet formation and reactivity of planar and faceted metal surfaces. We have continued successful collaborations with experimentalists at Princeton University (formerly at Lehigh University) who have made great contributions to the understanding of nanostructured Pt monolayer electrocatalyst.

I. 2. Details of Results

Our earlier studies related to this work have been documented in a few review articles.[1-5] Below we will summarize the main results obtained since our last three-year report on surface morphology and structure, surface chemistry and electrochemistry, growth of metallic nanoclusters and synthesis of nanoscale model electrocatalyst. The well-defined facet planes allow for detailed experimental and theoretical characterization and thus serve as nanoscale model catalysts and electrocatalysts to bridge the materials gap between planar metal single crystal surfaces and supported metal particles.

I.2.1. Adsorbate-induced Faceting of Metal Surfaces

I.2.1.A. Faceting of Re($11\bar{2}1$)

Reversible Transitions among Various Morphologies of Faceted Re($11\bar{2}1$). We have finished a detailed study of oxygen-induced faceting of Re($11\bar{2}1$) in a wide range of oxygen coverage and sample temperature using LEED, AES and STM.[6] The clean Re($11\bar{2}1$) surface is stable against faceting upon annealing up to 2000K. However, oxygen can induce faceting of Re($11\bar{2}1$), and the morphology of the faceted surface depends on the surface preparation conditions. We have discovered an unusual morphological evolution sequence on Re($11\bar{2}1$) as a function of surface oxygen coverage. Upon being exposed to O_2 at 300K followed by annealing in UHV at elevated temperatures, which results in a relatively low oxygen coverage, an initially planar Re($11\bar{2}1$) surface becomes partially faceted with zigzag chains formed by $(01\bar{1}0)$ and $(10\bar{1}0)$ facets coexisting with ($11\bar{2}1$) terraces, as shown in Figure I.1. At intermediate oxygen coverage, two meta-stable facets of $(33\bar{6}4)$ and (2×1) reconstructed $(11\bar{2}2)$ are formed corresponding to two different oxygen coverages. At high oxygen coverage obtained by dosing Re($11\bar{2}1$) with a large amount of O_2 on Re($11\bar{2}1$) at elevated temperatures, the surface becomes fully faceted exposing four facets of $(01\bar{1}0)$, $(10\bar{1}0)$, $(01\bar{1}1)$ and $(10\bar{1}1)$. A schematic of the

morphological transitions of oxygen-covered faceted Re(11$\bar{2}$1) is shown in Figure I.2. The models reveal that each facet contains micro-features that resemble the next facet phase in the morphological evolution sequence, which illustrates a natural connection among different structures of the facets. When annealing the oxygen-covered faceted surface in UHV, leading to a decrease in oxygen coverage due to partial desorption of oxygen, the morphology of Re(11$\bar{2}$1) transforms to the one at lower oxygen coverage. *This is the first observation of reversible morphology changes on a faceted metal single crystal surface under UHV conditions.* Our findings provide microscopic insights into the pathways of mass transport in oxygen-induced reversible morphologic transformation of faceted rhenium surfaces. This motivates a more detailed future exploration of oxygen-induced morphology transitions on catalytically active metal single crystal surfaces, which is of importance for design and development of new catalysts operating under oxygen-rich conditions since the shape (morphology) of supported metal nanoparticles varies with reaction conditions.[7-9]

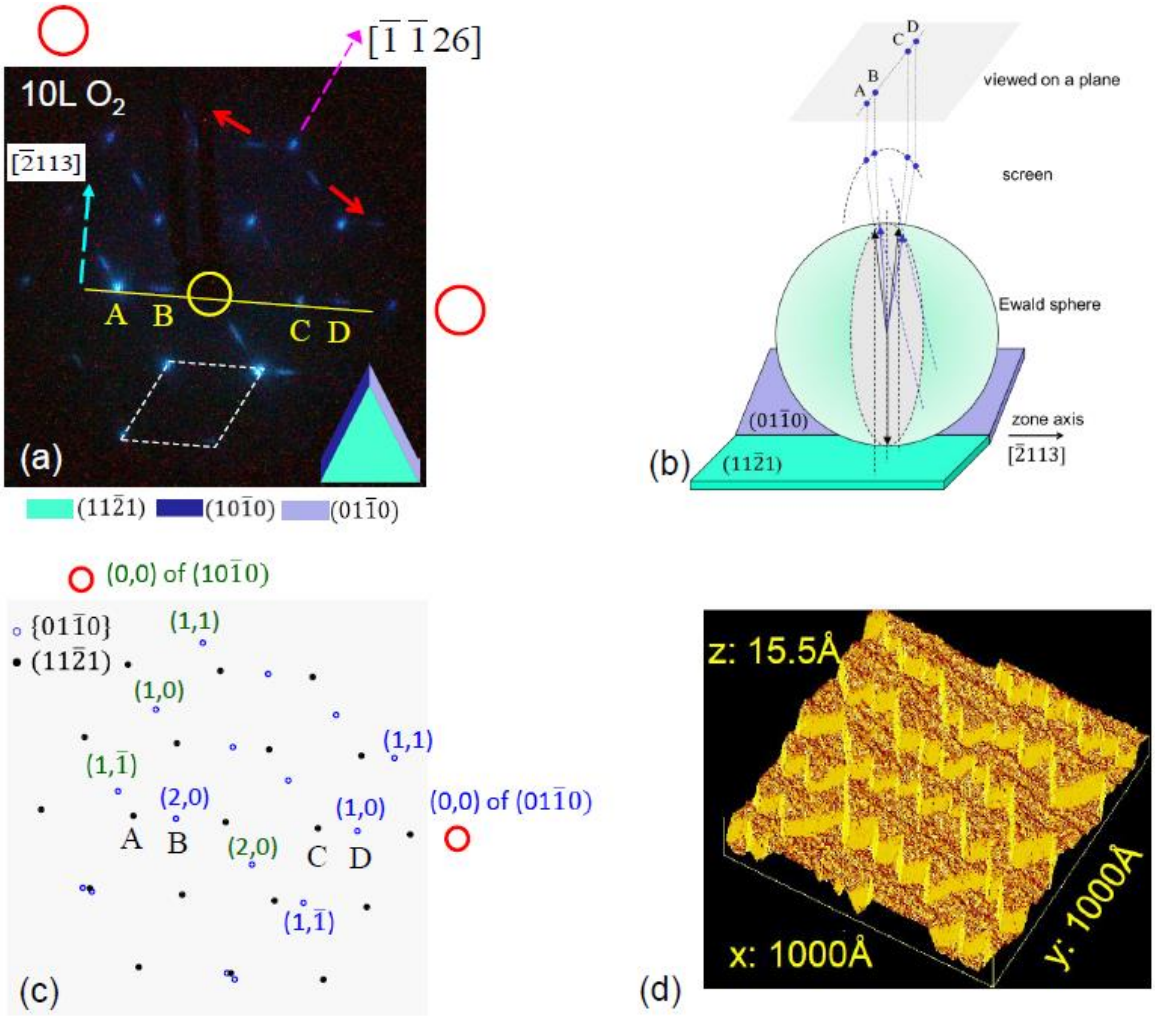

Figure I.1. (a) LEED pattern taken at 68 eV from a partially faceted Re(11$\bar{2}$1) after it is exposed to 10L O_2 at 300K followed by annealing at 1000K for 2min. The inset in the lower right corner shows a schematic model of the corresponding surface morphology. (b) Schematic diagram of the Edwald-sphere construction corresponding to the diffraction spots A-D in (a). (c) Kinematic LEED

simulation of (a) based on the 2D lattices of $(11\bar{2}1)$, $(01\bar{1}0)$ and $(10\bar{1}0)$, in which the solid circles are diffraction spots from $(11\bar{2}1)$ and the hollow circles are from $(01\bar{1}0)$ and $(10\bar{1}0)$. (d) 3D representation of the partially faceted surface showing the zigzag chains made of narrow bands of well-defined facets.

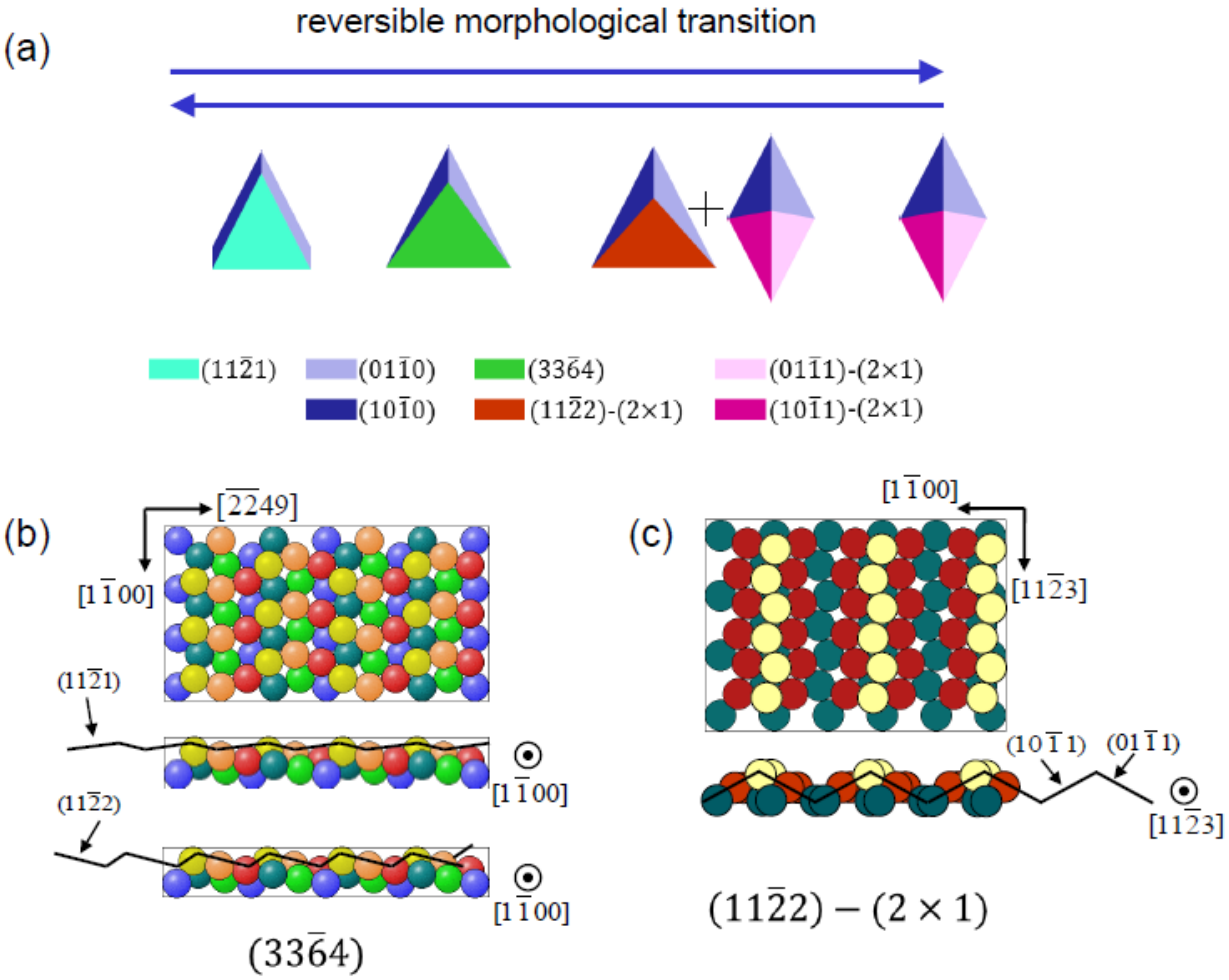

Figure I.2. (a) Schematic models of all the observed faceted structures on Re$(11\bar{2}1)$. (b) Hard-sphere model of the $(33\bar{6}4)$ facet. The side view shows two different ways of viewing the same surface. (c) Proposed hard-sphere model of the $(11\bar{2}2)$-(2×1) facet.

Experimental Studies of Carbon-induced Faceting of Re$(11\bar{2}1)$. We have initiated and performed a detailed study of carbon-induced faceting of Re$(11\bar{2}1)$ using XPS, AES, LEED and STM.[10] The motivation stems from two facts: 1) carbon-metal interaction has been studied extensively in recent years because of its importance in catalysis, nanotechnology, and synthesis of carbon nanotube and graphene,[11-16] 2) carbon in various forms has been used as catalyst and catalyst support.[11] We have searched for conditions for faceting to occur by varying exposures to C_2H_2 and sample temperatures in a wide range. We find that upon C_2H_2 exposure at elevated temperatures, an initially planar Re$(11\bar{2}1)$ surface becomes fully faceted and covered by carbon. The faceted surface is composed of three-sided pyramids exposing $(01\bar{1}1)$, $(10\bar{1}1)$ and $(11\bar{2}0)$

facets, as shown in Figure I.3. This morphological transformation occurs only at low C_2H_2 exposures (0.3 – 6.0 L) and temperature ≥ 800K.[17] Kinematical simulations of the experimentally observed LEED patterns from the faceted surface have been used to determine the facet orientations, which are then confirmed by STM measurements. *This is the first observation of C-induced faceting of an hcp metal single crystal surface and also the first real space observation of C-induced nano-faceting of metal single crystal surface.*

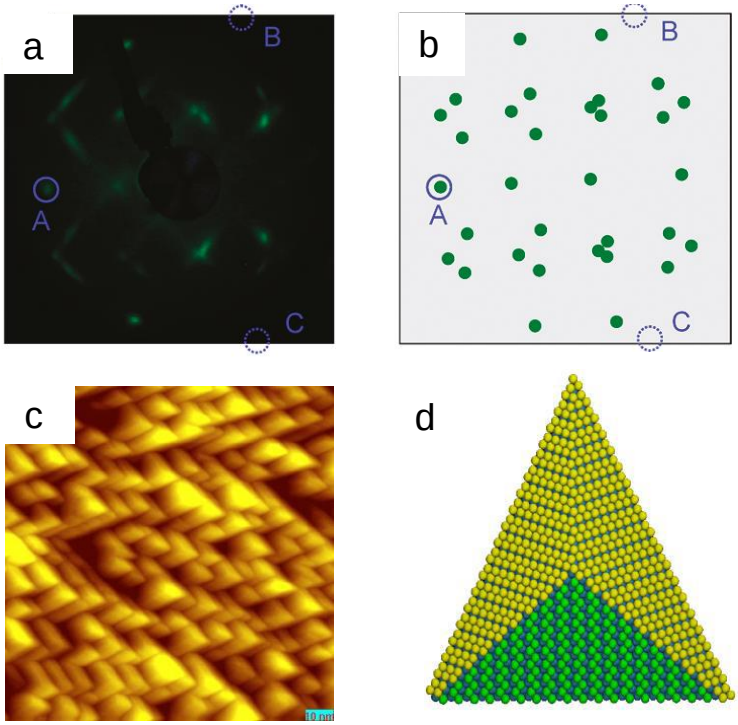

Figure I.3. (a) LEED pattern at 60eV from a faceted C/Re($11\bar{2}1$) surface prepared by dosing 0.3L of C_2H_2 at 700K followed by annealing at 1100K; (b) kinematical simulation of (a); (c) STM image from the same surface as (a); (d) hard sphere model of a single pyramid from the faceted Re($11\bar{2}1$) surface.

Theoretical Studies on Carbon-induced Faceting of Re($11\bar{2}1$). Using DFT in combination with the *ab initio* atomistic thermodynamics approach,[18] we have searched for the most stable structures for C on Re surfaces of planar $(11\bar{2}1)$ as well as $\{10\bar{1}1\}$ and $(11\bar{2}0)$ facets that form three-sided pyramids on the faceted surface.[17] We have investigated the binding sites and binding energies for C on Re surfaces with varying C coverages. We find that at low to intermediate coverage (0.25 – 1.0 GML) C atoms prefer binding at four-fold hollow sites on all studied Re surfaces. However, at high coverage (2.0 GML), three-fold hollow sites are occupied in addition to the four-fold hollow sites. Here, GML refers to geometrical monolayer, which is defined as the number of C atoms per (1×1) unit cell of the surface. Using the calculated total energies for C/Re surfaces including the substrate and the facets with different C coverages, we then studied the stability of clean and carbon-covered Re surfaces of planar $(11\bar{2}1)$ as well as facets at different C coverage, which enables construction of a surface phase diagram of C/Re surfaces. The calculations confirm the experimental findings that formation of three-sided

pyramidal facets is thermodynamically favored only at low carbon coverage as shown in Figure I.4.

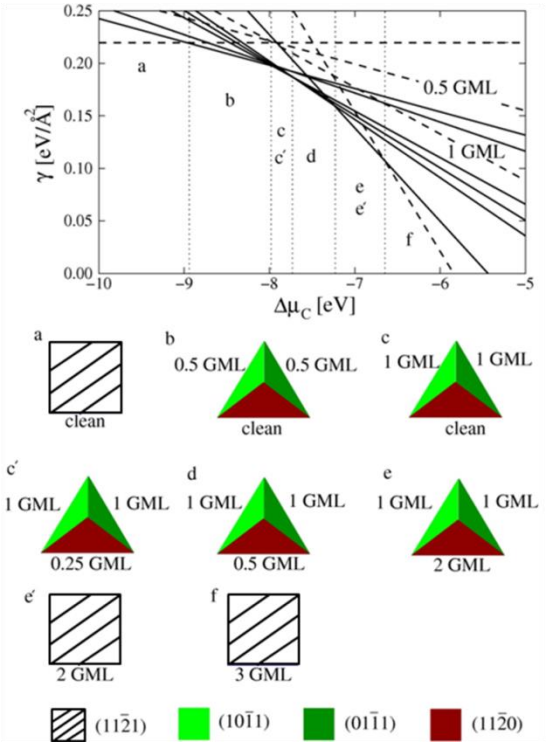

Figure I.4. Surface phase diagram for C-induced faceting of Re($11\bar{2}1$) showing the surface free energy of planar and faceted surfaces as a function of the carbon chemical potential.

Nitrogen-induced Reconstruction and Faceting of Re($11\bar{2}1$). We have carried out a detailed study on N-induced reconstruction and faceting of Re($11\bar{2}1$) by annealing in NH_3 with a wide range of NH_3 pressure and sample temperature.[19] The motivation is based on the fact that ammonia synthesis is highly structure sensitive on Re single crystal surfaces and a reactivity ratio of 1:94:920:2820 was found for Re(0001), Re($10\bar{1}0$), Re($11\bar{2}0$) and Re($11\bar{2}1$).[20] It has been shown that the first step in the ammonia synthesis is adsorption of nitrogen on the metal surfaces.[21, 22] We find that no reconstruction or faceting exists on the clean Re($11\bar{2}1$) surface, which is planar even after being annealed at temperatures up to 2000K: a (1×1) pattern is always observed in LEED. Upon dosing 100L NH_3 at 700K, the Re($11\bar{2}1$) surface develops a (2×1) reconstruction but still remains planar. When dosing 100L NH_3 on Re($11\bar{2}1$) at 900K, the (2×1) reconstruction disappears and the surface becomes fully faceted and covered by N, which consists of two-sided ridges formed by ($13\bar{4}2$) and ($31\bar{4}2$) facets as shown in Figure I.5. *This is the first observation of N-induced faceting of an hcp metal single crystal surface with well-defined facet structure and controlled nanoscale facet size.* The stability of high index planes of {$13\bar{4}2$} facets is attributed to the fact that {($13\bar{4}2$)} is vicinal to the {$10\bar{1}1$} surface that is more close-packed than ($11\bar{2}1$). The (2×1) substrate reconstruction is appearing in the sense that it can provide a natural link to the formation of {$13\bar{4}2$} facets. Figure I.5e shows a proposed model of a (2×1) substrate reconstruction of Re($11\bar{2}1$) which is made of two micro-facets. On the other hand, each {$13\bar{4}2$}

facet can be regarded as a stepped surface with terraces made of either of the same two micro-facets as shown in Figure I.5f. Thus the (2×1) reconstructed planar $(11\bar{2}1)$ surface can be regarded as a precursor state of faceting.

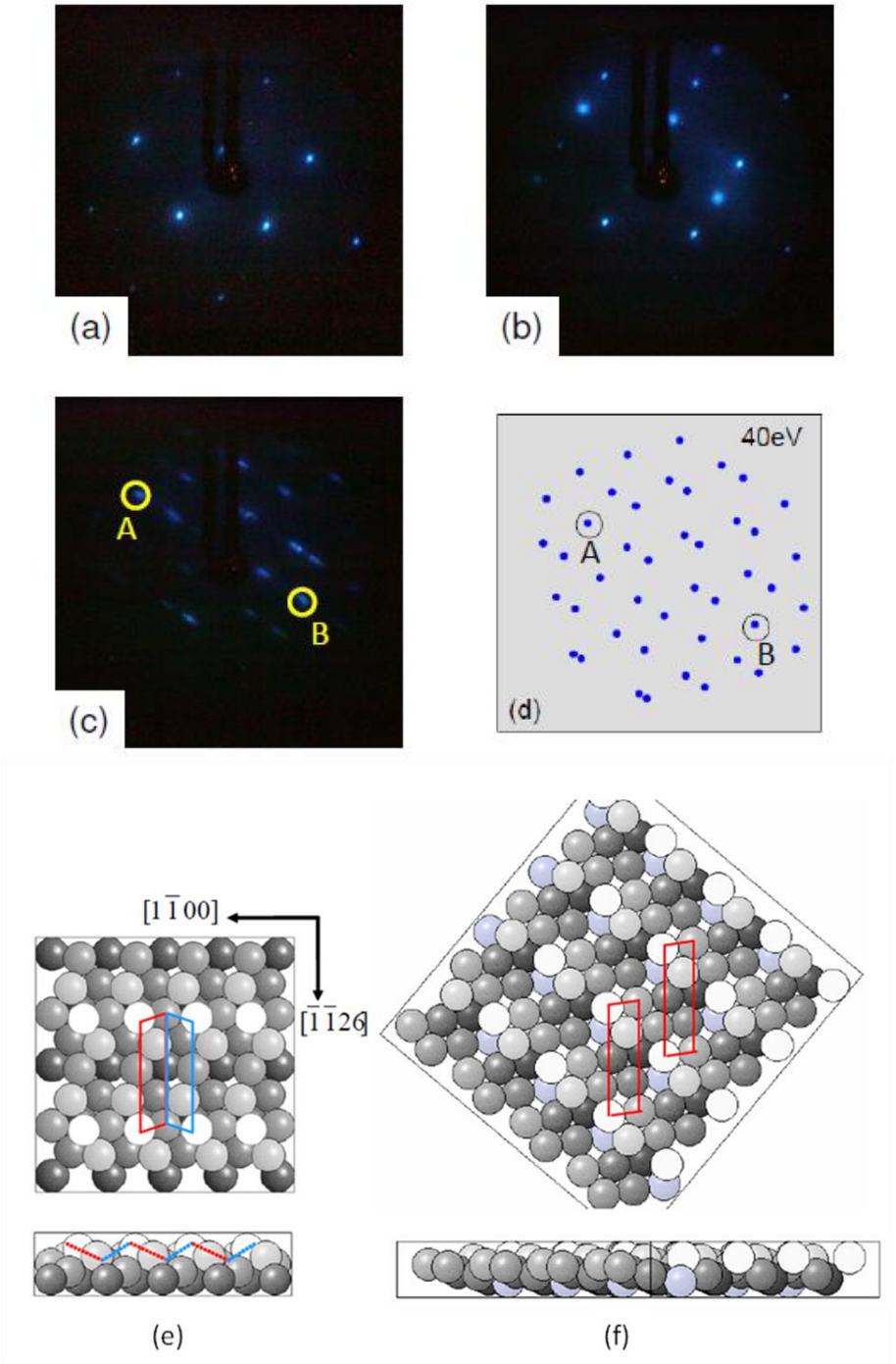

Figure I.5. LEED patterns taken at 40eV from clean Re$(11\bar{2}1)$ (a) and Re$(11\bar{2}1)$ after being exposed to 100L NH_3 at 700K (b) and 900K (c), respectively. (d) Kinematical LEED simulation of (c). (e) A proposed model for the (2×1) reconstructed $(11\bar{2}1)$ with every other row of atoms in the top layer along the $[1\,\bar{1}\,00]$ direction removed. The dash line in the side view show that this surface is made of two micro-facets; unit cells of the micro-facets are marked in the top view of the model. (f) The

$(13\bar{4}2)$ surface viewed as a stepped surface with terraces made of one of the micro-facets in (e); unit cells of two adjacent terraces are marked.

Surface Phase Diagram of N on Re Surfaces of $(11\bar{2}1)$ and Facets. Using DFT in combination with the *ab initio* atomistic thermodynamics approach,[18] we have determined the atomic geometries and energetics of N-covered Re surfaces of planar $(11\bar{2}1)$ as well as $\{13\bar{4}2\}$ facets that form two-sided ridges on the faceted surface.[17] We have investigated the binding sites and binding energies for N on the Re surfaces with varying N coverage Θ_N in GML (geometrical monolayer, which is defined as number of N atoms per (1×1) surface unit cell). The energetically most favorable structure at a given coverage of N on the Re surface is the one with the largest average binding energy (BE). The adsorption of N on Re$(13\bar{4}2)$ for coverage ranging from 1.0 to 6.0 GML shows almost comparable surface adsorbate densities as those on Re$(11\bar{2}1)$ with coverage ranging from 1.0 to 3.0 GML. For all studied Θ_N the binding energy of N on Re$(13\bar{4}2)$ is much higher than that on Re$(11\bar{2}1)$, which supports the stability of $(13\bar{4}2)$ facets on the Re$(11\bar{2}1)$ surface. We then studied the stability of clean and nitrogen-covered Re surfaces of $(11\bar{2}1)$ and facets through surface phase diagram of N/Re surfaces as shown in Figure I.6, which indicates that nitrogen adsorption causes two-sided ridges combining $(13\bar{4}2)$ and $(31\bar{4}2)$ facets to become thermodynamically favored at temperature below 1080K.

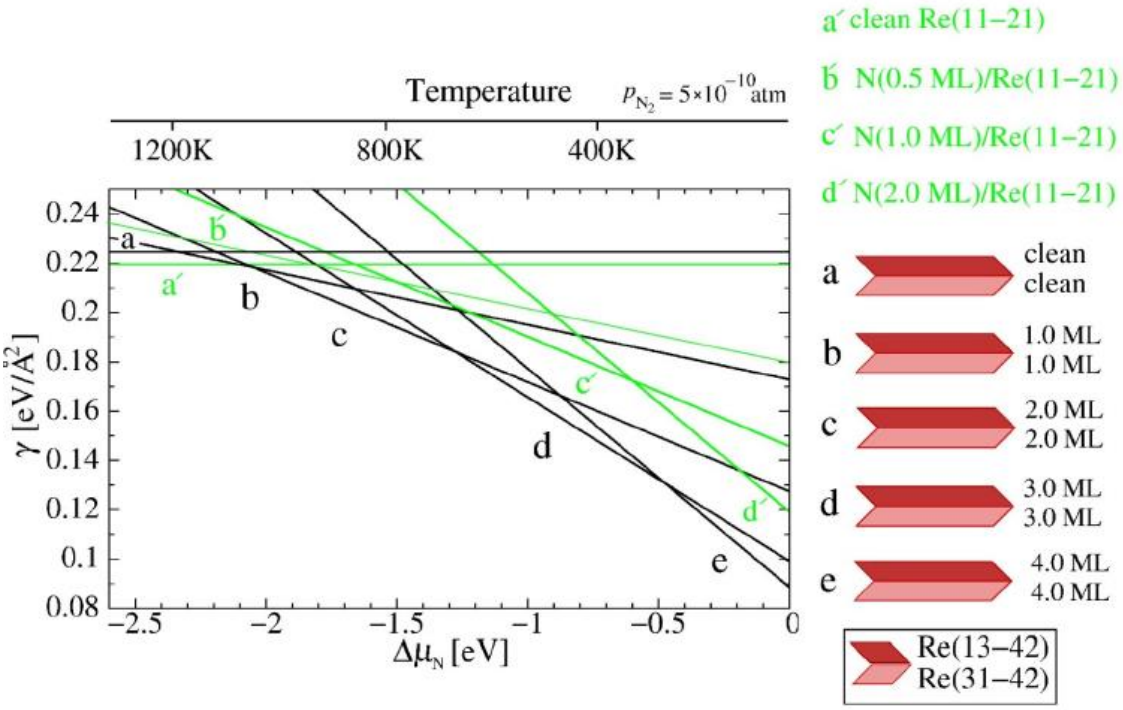

Figure I.6. Surface phase diagram for N-induced faceting of Re$(11\bar{2}1)$ showing the surface free energy of planar and faceted surfaces as function of the nitrogen chemical potential.

I.2.1.B. Faceting of Re$(12\bar{3}1)$

Carbon-induced Faceting of Re$(12\bar{3}1)$. We have initiated a study of C-induced faceting of Re$(12\bar{3}1)$ for comparison with C-induced faceting of Re$(11\bar{2}1)$.[23] Our preliminary LEED and AES results show that upon annealing in C_2H_2 at elevated temperatures, an initially planar Re(

$12\bar{3}1$) surface becomes fully faceted and covered by C. The faceted surface consists of two-sided ridges formed by two facets that have been determined as $(11\bar{2}0)$ and $(01\bar{1}1)$ by comparison of the kinematical simulations of LEED patterns with experimentally observed LEED patterns at various incident electron beam energy from the faceted surface. Figure I.7 shows a typical LEED pattern from the faceted C/Re($12\bar{3}1$) and a corresponding simulated LEED pattern. The faceted C/Re($12\bar{3}1$) surface is a promising nanotemplate for synthesis of metal monolayer electrocatalysts. The detailed exploration of surface morphology and facet size distribution of faceted C/Re($12\bar{3}1$) in real space will be the subject of a future study as described in Section II (Renewal Proposal).

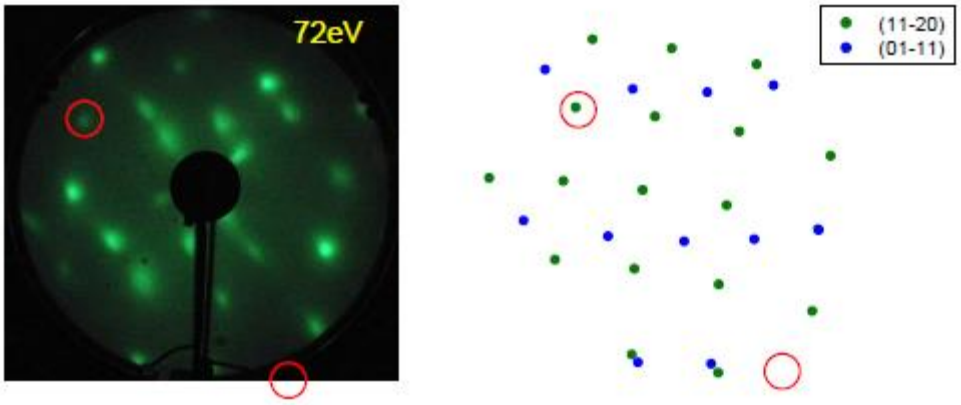

Figure I.7. (a) LEED pattern at 72 eV from a faceted C/Re($12\bar{3}1$) surface; (b) kinematical LEED simulation of (a).

I.2.1.C. Faceting of Ru($11\bar{2}1$)

Oxygen-induced Faceting of Ru($11\bar{2}1$). We have performed detailed studies on oxygen-induced faceting of Ru($11\bar{2}1$) by means of AES, LEED and STM[24] for comparison with oxygen-induced faceting of Ru($11\bar{2}0$).[25] The planar Ru($11\bar{2}1$) surface transforms into a fully faceted surface covered by oxygen upon annealing in NO_2 (10^{-8} Torr) or O_2 (10^{-6} Torr) at $T \geq 600K$. The faceted surface consists of long and uniform ridges at T<900K. The ridges are formed by four facets $(10\bar{1}1)$, $(01\bar{1}1)$, $(10\bar{1}0)$, and $(01\bar{1}0)$, and the ridge size grows as the annealing temperature increases. Details of the facet structures and reconstructions have been observed. Figure I.8 shows X-slope STM images obtained from the same original STM image by differentiating the height along the X (Figure I.8a) and –X directions (Figure I.8b), respectively. Differentiating the height along the X (scanning) direction brings the left side of the ridges brighter, where $(10\bar{1}1)$ and $(10\bar{1}0)$ facets are arranged as marked by the boxes. Differentiating the height along the -X direction brings the right side of the ridges brighter, showing $(01\bar{1}1)$ and $(01\bar{1}0)$ facets are arranged as marked by the boxes. These results are important for understanding the reactivity of Ru-based catalysts operating under oxygen-rich conditions as these catalysts may experience shape transformation due to the formation of new facet planes.

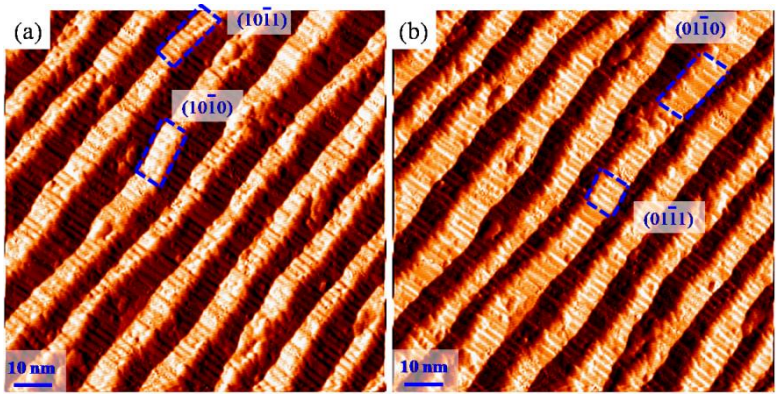

Figure I.8. X-slope STM images of oxygen-covered faceted Ru($11\bar{2}1$) obtained from the same original STM image by differentiating the height along X direction (scanning direction) (a) and –X direction (b). The faceted surface was prepared by exposing planar Ru($11\bar{2}1$) to 60L NO_2 at 883K.

Branching in Oxygen-induced Faceting of Ru($11\bar{2}1$**).** As described above, upon annealing in NO_2 at < 900K, oxygen-induced faceting of Ru($11\bar{2}1$) occurs, leading to formation of long and uniform ridges on the surface. However, when further increasing the annealing temperature to > 950K, branching of ridges was observed on the oxygen-covered faceted Ru($11\bar{2}1$) surface as shown in Figure I.9, in which wider ridges split into smaller ones.[26] *This is a surprising discovery and no previous report is found for branching on faceted metal single crystal surfaces.* The origin of branching on oxygen-covered faceted Ru($11\bar{2}1$) will be the subject of a future study as described in Section II (Renewal Proposal).

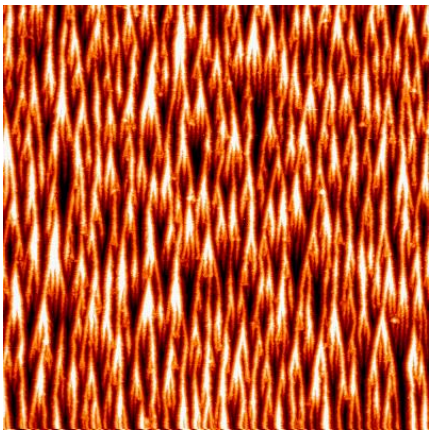

Figure I.9. STM image (500 nm×500 nm) of faceted O/Ru($11\bar{2}1$) by annealing in NO_2 at T > 950K.

Stability of Nitrogen-covered Ru($11\bar{2}1$**).** Motivated by N-induced faceting of Re($11\bar{2}1$) described above, we have carried out experiments to search for N-induced faceting of Ru($11\bar{2}1$) by annealing in NH_3 with varying exposures (up to 300L) and sample temperatures (from 550K to 1000K). We find that annealing Ru($11\bar{2}1$) in NH_3 does not induce faceting of Ru($11\bar{2}1$)) at all. Although the presence of the adsorbate does enhance the anisotropy of the surface free energy, which is the driving force for faceting, a sufficiently high sample temperature is required to

overcome kinetic barriers for surface atoms to diffuse and facilitate facet nucleate on, i.e. there are threshold (lowest) values of both adsorbate coverage and sample temperature for faceting to occur. It is well known that the sticking coefficient for dissociative adsorption of N_2 on Ru surfaces is very small,[27] and increased surface N coverage can be achieved by thermal decomposition of NH_3 on Ru. The absence of N-induced faceting of Ru$(11\bar{2}1)$ under our experimental conditions is attributed to an inability to reach the threshold values for both conditions at the same time. In other words, the lack of N-induced faceting of Ru$(11\bar{2}1)$ is attributed to an insufficient nitrogen coverage on the surface since TPD measurements from NH_3/Ru$(11\bar{2}1)$ show that nitrogen starts to desorb at 500K and completely desorbs from Ru$(11\bar{2}1)$ as N_2 at ~700K.[28]

I.2.2. Reactions on Planar and Nano-Faceted Metal Surfaces

Upon annealing in O_2 (5×10^{-8} Torr) at $T \geq 600$K, planar Ir(210) converts to oxygen-covered faceted Ir(210) that consists of three-sided pyramids exposing (110) and {311} facets. The morphology of faceted O/Ir(210) is independent of oxygen coverage, and the average pyramid size increases with annealing temperature from 5nm to 14nm while the facet structures on each pyramid remain unchanged.[29, 30] Clean faceted Ir(210) can be prepared *in situ* through reaction with H_2 at 400K to remove oxygen from faceted O/Ir(210) while facets retain their original structure and size, as shown in Figure I.10.[30, 31] The generation of clean faceted Ir(210) with tunable facet size on the nanometer scale is unprecedented on faceted metal surfaces, which have been used to explore size effects in chemical reactions.[30, 32-35] New results since the last three-year report are as follows.

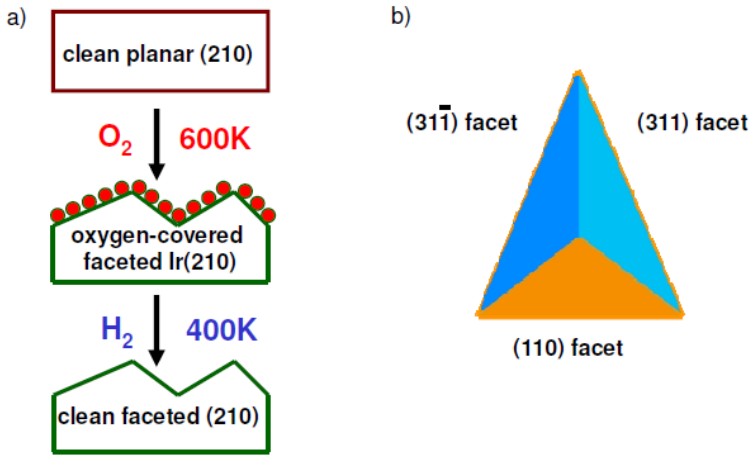

Figure I.10. (a) Schematic of the process to produce a clean faceted Ir(210) surface; (b) Schematic of a single pyramid from the faceted Ir(210) surface.

Reactivity and Reaction Pathway in Oxidation of CO by NO on Ir. We have finished investigating oxidation of CO by pre-adsorbed NO on planar Ir(210) and faceted Ir(210) with facet sizes of 5nm and 14nm.[31] Both clean planar Ir(210) and clean faceted Ir(210) favor oxidation of CO to CO_2, which is accompanied by simultaneous reduction of NO with high selectivity to N_2.

The TPD data indicate the same reaction pathway for CO_2 formation from oxidation of CO either by pre-adsorbed NO or by pre-adsorbed O on planar Ir(210), which infers that the former reaction on Ir(210) proceeds via reaction of CO with O that is generated by the decomposition of NO. Co-adsorbed CO affects dissociation of NO at low NO pre-coverage on Ir(210) but not at high NO pre-coverage on Ir(210). Planar Ir(210) is more active for CO_2 formation than faceted Ir(210) at low NO pre-coverage as evidenced by much lower onset temperature for CO_2 desorption and lower CO_2 desorption peak temperature on planar Ir(210) than those on faceted Ir(210), similar to oxidation of CO by pre-adsorbed oxygen at low O pre-coverage on Ir(210). Moreover, faceted Ir(210) with smaller facet size is more active for CO_2 formation from oxidation of CO by pre-adsorbed NO at low NO pre-coverage, in contrast to oxidation of CO by pre-adsorbed oxygen where no size effects were found. The much lower barrier (~0.1 eV) for O 1D diffusion along the … -T-D-B-D-T-… direction on Ir(210) than those on Ir(110) and Ir(311) as revealed by DFT calculation, resulting in rather mobile O atoms with high binding energy (BE) on Ir(210) (Figure I.11), may be the key to the higher reactivity of planar Ir(210) for formation of CO_2. *This work demonstrates the novelty of faceted Ir(210) in exploring structural and size effects in catalytic reactions. The size effects observed in this work exclude not only the influence of a support material but also effects that result from changes in catalyst morphology induced by the changes in particle size: two effects that are common to supported catalysts.*

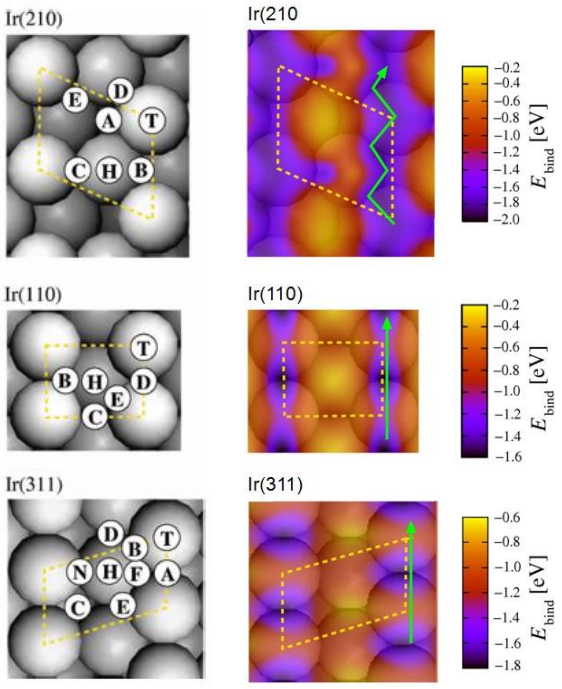

Figure I.11. (left panel) Top views of hard-sphere bulk truncation models of Ir(210), Ir(110), and Ir(311) showing possible adsorption sites. (right panel) Surface contour plots of the adsorption energy distribution (with respect to gas phase O_2) for binding 1 GML O onto the Ir(210), Ir(110) and Ir(311) surfaces.

TPD and DFT Studies of hydrogen adsorption and desorption on Ir. We have performed a detailed study of hydrogen adsorption and desorption on clean planar Ir(210) as well as clean faceted Ir(210), consisting of {311} and (110) facets with facet sizes of 5-14nm, by means of TPD and DFT in combination with the *ab initio* atomistic thermodynamics approach.[36]

Hydrogen dissociatively adsorbs on Ir surfaces at 300K. TPD spectra exhibit only one H_2 peak from planar Ir(210) at all coverages, whereas on faceted Ir(210) a single H_2 peak is observed at around 440K (F1) at fractional monolayer (ML) coverage and an additional H_2 peak appears at around 360K (F2) at 1 ML, implying structure sensitivity in recombination and desorption of hydrogen on faceted Ir(210) versus planar Ir(210), as shown in Figure I.12 (top panel). However, no evidence is found for size effects in recombination and desorption of hydrogen on faceted Ir(210) for average facet sizes of 5-14nm. Calculations indicate that H prefers to bind at the two-fold short-bridge sites on the Ir surfaces. In addition, we studied the stability of the Ir surfaces in the presence of hydrogen at different H coverage through surface free energy plots as a function of the hydrogen chemical potential as shown in Figure I.12 (bottom panel). The calculations revealed the origin of the two H_2 peaks from faceted Ir(210) observed in TPD: F1 is from desorption of hydrogen on {311} facets while F2 is from desorption of hydrogen on (110) facets. *This work has been published in Physical Chemistry Chemical Physics (2013) and was commented by the referee as "This paper is an excellent example of high level research where experiment and theory go together".*

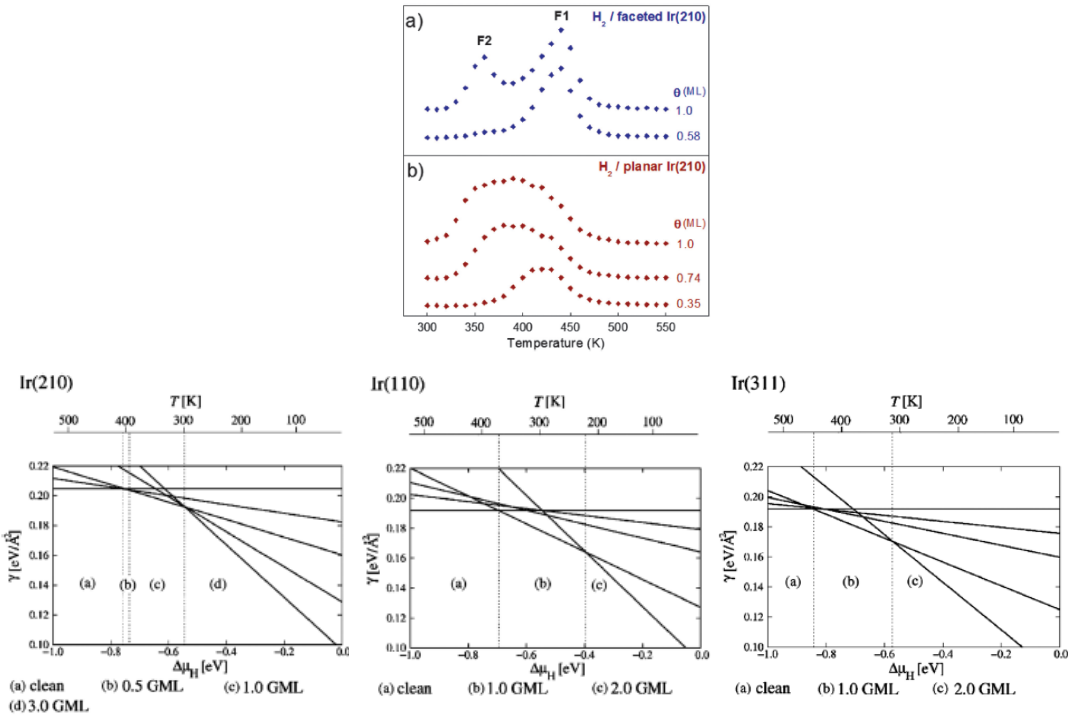

Figure I.12. (top panel) TPD spectra of H_2 from faceted Ir(210) and planar Ir(210) surfaces pre-dosed with H_2 at 300K; (bottom panel) Surface phase diagrams for H on Ir surfaces showing the surface free energy as a function of the H chemical potential.

Reduction of Nitric Oxide by Acetylene on Planar and Faceted Ir(210). We have investigated reduction of NO by C_2H_2 on planar Ir(210) and faceted Ir(210) with different facet sizes (5nm and 14nm).[37] Upon adsorption on the Ir surfaces, C_2H_2 dissociates to form acetylide (CCH) and H species at low C_2H_2 pre-coverage.[38] For adsorption of NO on C_2H_2-covered Ir, both planar and faceted Ir(210) exhibit high reactivity for reduction of NO with high selectivity to N_2 at low C_2H_2 pre-coverage, while the reaction is completely inhibited at high C_2H_2 pre-coverage. Co-adsorbed C_2H_2 significantly influences NO dissociation. The N-, H- and C-containing reaction

products are dominated by N_2, H_2, CO and CO_2 together with a small amount of H_2O. For adsorption of NO on C-covered Ir(210) at fractional C pre-coverage, CO_2 formation is promoted while CO production is reduced (Figure I.13), *indicating the beneficial effects of surface carbon at fractional coverage on the selectivity to C-containing products in the reduction of NO*. Reduction of NO by C_2H_2 is structure sensitive on faceted Ir(210) versus planar Ir(210) (Figure I.14) but no evidence is found for size effects in this reaction on faceted Ir(210) for average facet sizes of 5nm and 14nm. The results are compared with reduction of NO by CO on the same Ir surfaces. Like the NO+C_2H_2 reaction, the Ir surfaces are very active for reduction of NO by CO with high selectivity to N_2 and the reaction is structure sensitive on faceted Ir(210) versus planar Ir(210), but clear evidence is found for size effects in the reduction of NO by CO on faceted Ir(210). Furthermore, co-adsorbed CO does not affect dissociation of NO at low CO pre-coverage whereas co-adsorbed CO considerably influences NO dissociation at high CO pre-coverage. Since this work shows the beneficial effects of sub-monolayer surface carbon on C-containing product selectivity in the reduction of NO, it merits further study using C-covered faceted metal surfaces as catalysts as described in Section II (Renewal Proposal).

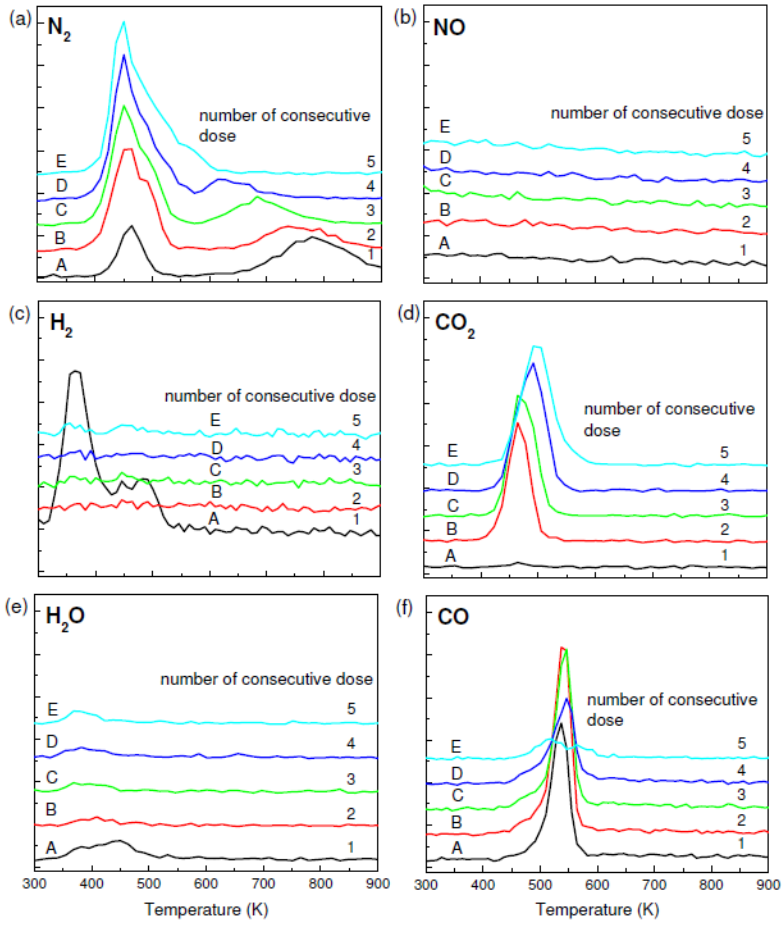

Figure I.13. TPD spectra of N_2, NO, H_2, CO_2, H_2O and CO from adsorption of consecutive dose of 0.5L NO on planar Ir(210) pre-exposed to 0.5L C_2H_2 at 300K.

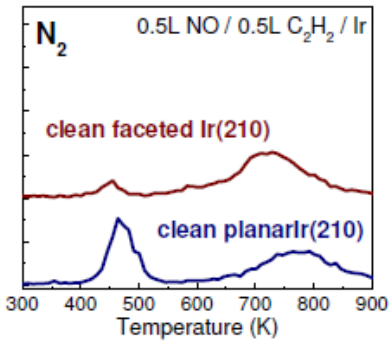

Figure I.14. TPD spectra of N_2 from adsorption of 0.5L NO on planar and faceted Ir(210) pre-covered by 0.5L C_2H_2.

Selective Oxidation of Ammonia on Planar and Faceted Ir(210). We have initiated and performed a detailed study on selective catalytic oxidation of ammonia by pre-adsorbed oxygen on planar and faceted Ir(210) using TPD under UHV conditions.[39] Selective catalytic oxidation of ammonia to nitrogen is potentially an ideal technology for removing ammonia from oxygen-containing waste gases, which has been extensively studied.[40-46] Iridium was found to be more active and selective to produce nitrogen than commonly used platinum.[41] Our TPD data from adsorption of ammonia on O-covered planar Ir(210) (Figure I.15) and faceted Ir(210) (Figure I.16) show the evidence for formation of N_2O from both surfaces. *This is the first observation of N_2O formation in catalytic ammonia oxidation under UHV conditions (< 1×10^{-9} Torr).* The selectivity of the reaction to N_2, N_2O and NO can be tuned by oxygen pre-coverage, surface structure and facet size. The reaction exhibits strong structure sensitivity on faceted Ir(210) versus planar Ir(210) and moderate size effects on faceted Ir(210) for average facet sizes of 5-14nm. On planar Ir(210), at low oxygen pre-coverage, only N_2 is produced. Formation of N_2 and N_2O is detected at intermediate oxygen coverage. High oxygen coverage leads to formation of N_2, N_2O and NO. The observation of N_2O is a surprising finding because formation of N_2O from ammonia oxidation was often observed under high pressure reactions but was not detected under UHV conditions. We will perform HREELS measurements of ammonia oxidation by pre-adsorbed oxygen on planar and faceted Ir(210) to identify the reaction intermediates and reaction pathways, which will be the subject of a future study as described in Section II (Renewal Proposal).

Adsorption Sites of CO, O, H, NO, CO+O, CO+NO and CCH+H on Ir. We have determined the energetically preferred binding sites and binding energies (BEs) of CO, O, H, NO, CO+O, NO+CO and CCH+H on Ir(210) as well as on Ir(311) and Ir(110), which are involved in the formation of three-sided pyramidal facets on Ir(210), using DFT.[31, 36, 37] The results enabled us to better understand reactivity of planar and faceted Ir(210) in catalytic reactions of CO oxidation by pre-adsorbed oxygen and NO, reduction of NO by pre-adsorbed CO and acetylene, and adsorption and desorption of hydrogen.

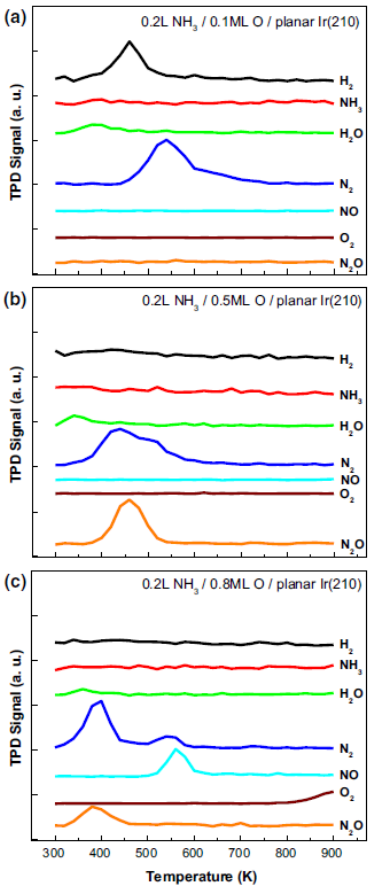

Figure I.15. TPD spectra from adsorption of 0.2L NH_3 on planar Ir(210) pre-exposed to 0.2L O_2 (~0.1 ML O), 1L O_2 (~0.5 ML O) and 5L O_2 (~0.8 ML O), respectively, at 300K.

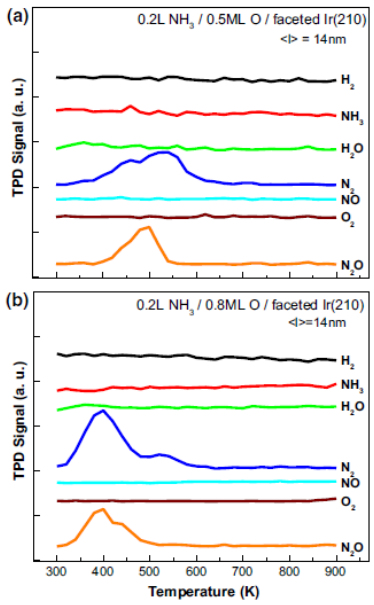

Figure I.16. TPD spectra from adsorption of 0.2L NH_3 on faceted Ir(210) (with average facet size of 14nm) pre-exposed to 1L O_2 (~0.5 ML O) and 5L O_2 (~0.8 ML O), respectively, at 300K.

I.2.3. Nanotemplates For Synthesis of Nanoclusters and Nanoscale Model Electrocatalyst

Growth of Gold Nanoclusters on Faceted O/Ru. We have completed detailed studies on the growth of Au nanoclusters over oxygen-covered faceted Ru($11\bar{2}0$) by AES, LEED and STM.[47] Ru($11\bar{2}0$) becomes fully faceted and covered by oxygen upon annealing in NO_2 at elevated temperatures, and the faceted O/Ru($11\bar{2}0$) surface consists of parallel and uniform ridges along the [0001] direction with dimensions ~6nm wide and >200nm long, which are formed by four {$01\bar{1}1$} facets.[25] Using the faceted O/Ru($11\bar{2}0$) surface as a nanotemplate, preferential nucleation and growth of gold nanoclusters has been achieved. Deposition of gold onto the nanotemplate at room temperature without post annealing leads to formation of gold nanoclusters that are spaced regularly and have a narrow size distribution, as shown in Figure I.17. This is in contrast to growth of Co nanoclusters on faceted O/Re($12\bar{3}1$), which requires post annealing.[48] Gold nanoclusters nucleate and grow preferentially within troughs of the ridges on faceted O/Ru($11\bar{2}0$) and their size can be controlled by changing gold coverage. *Our work demonstrates that faceted metal surfaces are excellent nanotemplates for synthesis of metal nanoclusters at specific sites with narrow size distribution.*

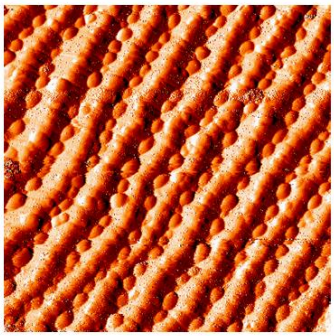

Figure I.17. X-slope STM image (50nm × 50nm) from deposition of 0.3ML Au on faceted O/Ru($11\bar{2}0$) at room temperature.

Synthesis of Pt Monolayer Electrocatalyst on Faceted C/Re($11\bar{2}1$). We have performed a detailed study of using the faceted C/Re($11\bar{2}1$) surface as a nanotemplate to synthesize Pt monolayer (ML) electrocatalyst. Pt is chosen based on the following two facts.[10] First, our earlier study showed no evidence for Pt-induced faceting of Re($12\bar{3}1$). This may be attributed to intermixing between Pt and Re, which was evidenced by our synchrotron-based HRXPS measurements (unpublished data). Therefore, Pt-induced faceting of Re($11\bar{2}1$) under our experimental conditions is unlikely. Second, the hydrogen evolution reaction (HER) is one of the most extensively studied electrochemical reactions,[49-54] and Pt is commonly used as an electrocatalyst for HER. Of particular interest is the use of Pt monolayer (ML) catalysts for the HER in order to substantially reduce the Pt loading.[50, 52] For example, it was found that the activity of a Pt ML supported on planar tungsten carbide (WC) shows the same HER activity as bulk Pt.[52] We have successfully synthesized a Pt ML electrocatalyst by depositing one physical ML of Pt onto the faceted C/Re($11\bar{2}1$) surface at room temperature, denoted as Pt ML/C/Re($11\bar{2}1$), as shown in Figure I.18a, whose activity for the HER has been tested and will be described below. The Pt coverage was characterized by both LEIS and XPS, as shown in Figures I.18b and I.18c. The LEIS spectrum in Figure I.18b from the Pt ML on faceted C/Re($11\bar{2}1$) (blue curve) displays

only a Pt peak and a negligible Re peak, whereas the red curve shows only a Re peak in the LEIS spectrum from the clean Re($11\bar{2}1$) surface.

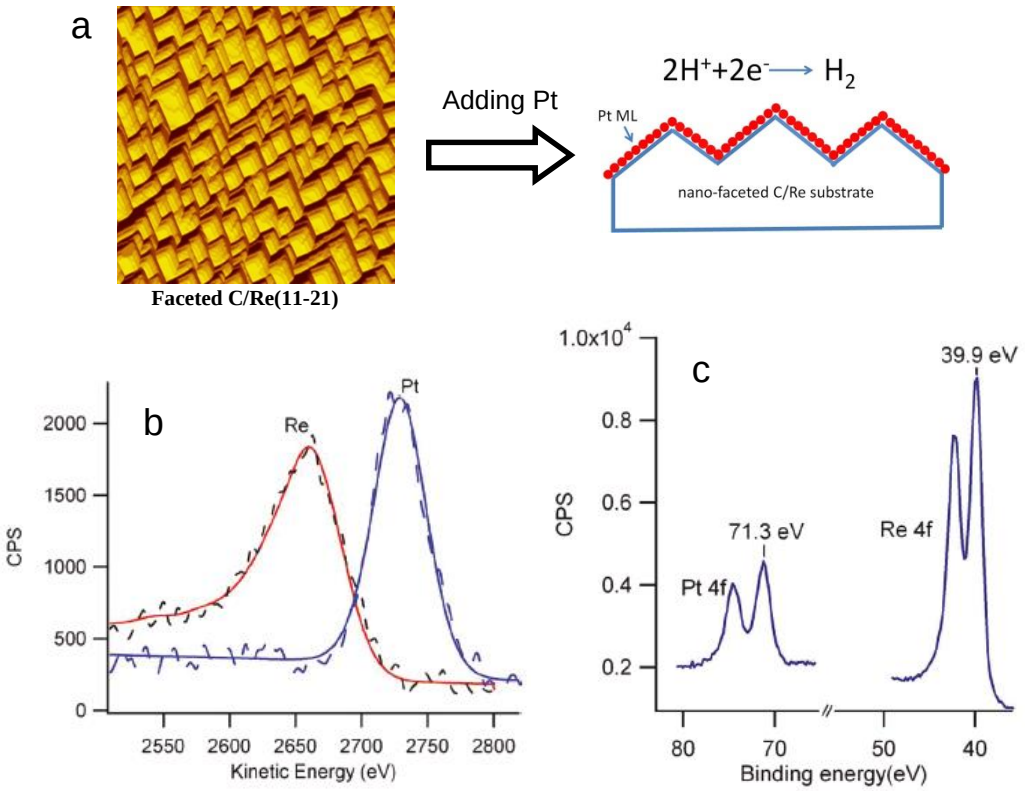

Figure I.18. (a) Schematic diagram of synthesizing Pt ML electrocatalyst on faceted C/Re($11\bar{2}1$). Surface characterization of a Pt ML supported on faceted C/Re($11\bar{2}1$) by LEIS (b) and XPS (c). In (b), the red curve was taken from a clean Re($11\bar{2}1$) surface.

Reactivity of Pt ML Supported on Faceted C/Re($11\bar{2}1$). After preparing a Pt ML supported on faceted Re($11\bar{2}1$), we have tested its reactivity for HER.[10] Figure I.19(left panel) shows polarization scans for the HER using Re($11\bar{2}1$), Pt(111), and Pt ML/C/Re($11\bar{2}1$) samples, which were performed in an Ar-purged 0.1 M $HClO_4$ solution at room temperature with a scan rate of 2mV/s. Figure I.19(right panel) gives plots of the HER overpotentials as a function of the logarithm of the exchange current density to produce the corresponding set of the Tafel curves. Clearly, the activity of Re($11\bar{2}1$) for the HER is much lower than Pt(111) as evidenced by the large overpotential. However, the Pt ML/C/Re($11\bar{2}1$) sample has a significantly improved activity with even better performance than Pt(111). The exchange current (j_0) values for Pt ML/C/Re($11\bar{2}1$) and Pt(111) are 6.30×10^{-4} and 3.98×10^{-4} A/cm^2, respectively. *This work is the first application of faceted metal surfaces as nanotemplates for synthesis of nanoscale model electrocatalyst with well-defined (facet) structure and controlled (facet) size on the nanometer scale,* which illustrates the potential for future studies of nanostructured bimetallic systems relevant to electrocatalytic reactions as described in Section II (Renewal Proposal).

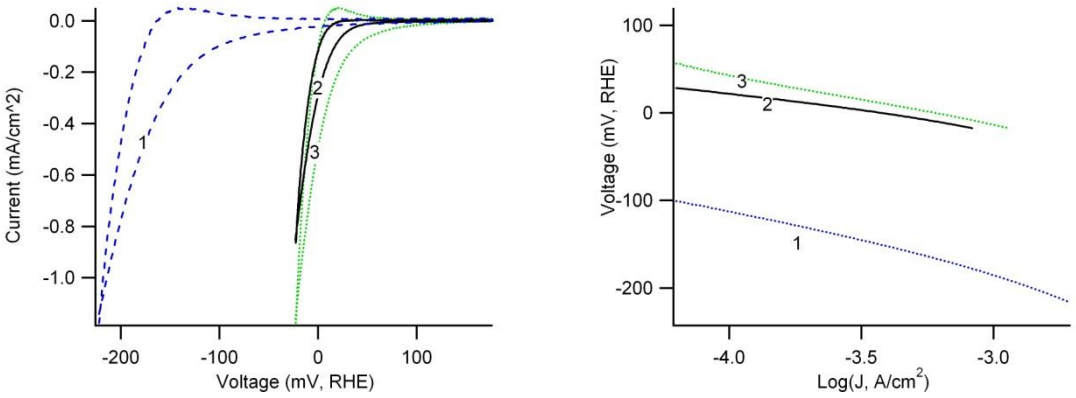

Figure I.19. (left panel) HER polarization curves of (1) Re($11\bar{2}1$), (2) Pt(111) and (3) Pt ML supported on faceted C/Re($11\bar{2}1$), in Ar-purged 0.1M $HClO_4$; and (right panel) corresponding Tafel plots for the data in (left panel). The scan rate in the polarization measurements was 2mV/s.

I. 3. Concluding Remarks

This report includes the first detailed studies on faceting of metal surfaces induced by adsorbate species (O, N, C) and their applications in catalysis and electrocatalysis. These results are important for environmental- and energy-related applications and help understand the mechanisms of possible dynamic structural rearrangements at the surfaces of highly dispersed metal catalysts under high temperature and pressure as well as clarify the role of structural and nanoscale size effects in catalysis and electrocatalysis under operating conditions.

As indicated above, these activities are enhanced by collaborations through which the DOE funds are considerably leveraged. The factor that distinguishes this work from other studies of model metal catalysts is our emphasis on atomically rough and high surface energy surfaces that are morphologically unstable during reaction conditions. Our work leads to fabrication of nanoscale model heterogeneous catalysts as well as nanoscale model electrocatalysts with well defined facet structure and controllable facet size on the nanometer scale, which bridges the materials gap between metal single crystal surfaces and supported metallic nanoparticles in catalysis and electrocatalysis.

I. 4. Publications since Last Three-year Report

Sole funding by DOE and this grant

1) "Reduction of NO by CO on unsupported Ir: Bridging the materials gap", W. Chen, Q. Shen, R.A. Bartynski, P. Kaghazchi and T. Jacob, ChemPhysChem **11**, 2515 (2010). (*featured on the front cover and highlighted in the news section of ChemPhysChem*)

2) "Growth of gold nanoparticles on faceted O/Ru($11\bar{2}0$) nanotemplate", Q. Shen, W. Chen and R.A. Bartynski, Surf. Sci. **605**, 1457 (2011).

3) "Nano-faceted C/Re($11\bar{2}1$): fabrication, structure and template for synthesizing nanostructured model Pt electrocatalyst for hydrogen evolution reaction", X. Yang, B.E. Koel, H. Wang, W. Chen*, and R.A. Bartynski, ACS Nano **6**, 1404 (2012).

4) “Oxidation of CO by NO on planar and faceted Ir(210)”, W. Chen, R.A. Bartynski, P. Kaghazchi and T. Jacob, J. Chem. Phys. **136**, 224701 (2012).

5) “New surfaces stabilized by adsorbate-induced faceting”, P. Kaghazchi, T. Jacob, I. Ermanoski, W. Chen and T. E. Madey, J. Phys.: Condens. Matter **24**, 265003 (2012).

6) “Reduction of nitric oxide by acetylene on Ir surfaces with different morphologies: comparison with reduction of NO by CO”, W. Chen, Q. Shen, R.A. Bartynski, P. Kaghazchi and T. Jacob, Langmuir **29**, 1113 (2013).

7) “Theoretical and experimental studies of hydrogen adsorption and desorption on Ir surfaces”, P. Kaghazchi, T. Jacob, W. Chen and R.A. Bartynski, Phys. Chem. Chem. Phys. **15**, 12815 (2013). (*commented by the referee as “This paper is an excellent example of high level research where experiment and theory go together”*)

8) “Morphological stability of oxygen- and nitrogen-covered Ru($11\bar{2}1$)”, Q. Shen, W. Chen, H. Wang and R.A. Bartynski, J. Chem. Phys. **139,** 084707 (2013).

9) “Theoretical and experimental studies on carbon-induced faceting of Re($11\bar{2}1$)”, P. Kaghazchi, T. Jacob, X. Yang, G. Junno, H. Wang, W. Chen, B.E. Koel and R.A. Bartynski, Catal. Lett. **144**, 1667 (2014).

10) “Nitrogen-induced reconstruction and faceting of Re($11\bar{2}1$)”, H. Wang, W. Chen, R.A. Bartynski, P. Kaghazchi and T. Jacob, J. Chem. Phys. **140**, 024707 (2014).

11) “Selective oxidation of ammonia by co-adsorbed oxygen on iridium surfaces: Formation of N_2O”, W. Chen, Q. Shen and R.A. Bartynski, Catal. Lett. **145**, 757 (2015).

12) “Oxygen-induced nano-faceting of Re($11\bar{2}1$)”, H. Wang, W. Chen and R.A. Bartynski, Surf. Sci. **635**, 85 (2015).

13) “Nanofaceted metal surfaces: Structure, reactivity and applications”, W. Chen, H. Wang and R.A. Bartynski, in: Z. Wu and S.H. Overbury (Eds), Catalysis by Materials with Well-defined Structures, Elsevier B.V. (ISBN: 978-0-12-801217-8), Chapter 11 (pp. 301-338), 2015. (*invited review paper as a chapter for the book*)

14) “Carbon-induced faceting of Re($12\bar{3}1$)”, H. Wang, Q. Shen, W. Chen and R.A. Bartynski, in preparation.

15) “Branching in oxygen-induced faceting of Ru($11\bar{2}1$)”, Q. Shen, W. Chen, H. Wang, and R.A. Bartynski, in preparation.

Joint funding by DOE and other federal or non-federal sources

16) “Interaction of benzene and toluene vapors with Ru(0001) surface: relevance to MLM contamination”, B.V. Yakshinskiy, Q. Shen and R.A. Bartynski, Proc. SPIE **7969**, 796922 (2011).

17) “Evidence for the collapse of short-range magnetic order in CoO at the Néel temperature”, R. Gotter, F. Offi, A. Ruocco, F. Da Pieve, R. Bartynski, M. Cini and G. Stefani, EPL **94**, 37008 (2011).

18) “Conversion reaction of FeF_2 thin films upon exposure to atomic lithium”, S. Rangan, R. Thorpe, R.A. Bartynski, M. Sina, F. Cosandey, O. Celik and D.D.T. Mastrogiovann, J. Phys. Chem. C **116**, 10498 (2012).

19) “Increasing photocurrents in dye sensitized solar cells with tantalum-doped titanium oxide photoanodes obtained by laser ablation”, R. Ghosh, H. Yukihiro, L. Alibabaei, K. Hanson, S. Rangan, R. Bartynski, T.J. Meyer and R. Lopez, ACS Appl. Mater. Interfaces **4**, 4566 (2012).

20) “Spin-dependent on-site electron correlations and localization in ltinerant ferromagnets”, R. Gotter, G. Fratesi, R.A. Bartynski, F. Da Pieve, F. Offi, A. Ruocco, S. Ugenti, M.I. Trioni, G.P. Brivio and G. Stefani, Phys. Rev. Lett. **109**, 126401 (2012).

21) “Energy alignment, molecular packing, and electronic pathways: Zinc(II) tetraphenylporphyrin derivatives adsorbed on TiO_2(110) and ZnO($11\bar{2}0$) surfaces”, S. Rangan, S. Coh, R.A. Bartynski, K.P. Chitre, E. Galoppini, C. Jaye and D. Fischer, J. Phys. Chem. C **116**, 23921 (2012).

22) “A sensitized Nb_2O_5 photoanode for hydrogen production in a dye-sensitized photoelectrosynthesis cell”, H. Luo, W. Song, P.G. Hoertz, K. Hanson, R. Ghosh, S. Rangan, M.K. Brennaman, J.J. Concepcion, R.A. Binstead, R.A. Bartynski, R. Lopez and T.J. Meyer, Chem. Mater. **25**, 122 (2013).

23) “Conversion reaction of CoO polycrystalline thin films exposed to atomic lithium”, R. Thorpe, S. Rangan, M. Sina, F. Cosandey and R.A. Bartynski, J. Phys. Chem. C **117**, 14518 (2013).

24) “Energy level alignment of polythiophene/ZnO hybrid solar cells”, W. Feng, S. Rangan, Y. Cao, E. Galoppini, R.A. Bartynski and E. Garfunkel, J. Mater. Chem. A **2**, 7034 (2014).

25) “Band gap of epitaxial in-plane-dimerized single-phase NbO_2 films”, A.B. Posadas, A. O´ Hara, S. Rangan, R.A. Bartynski and A.A. Demkov, Appl. Phys. Lett. **104**, 092901 (2014).

26) “Tuning energy level alignment at organic/semiconductor interface using a built-in dipole in Chromophore-bridge-anchor compounds”, S. Rangan, A. Batarseh, K.P. Chitre, A. Kopecky, E. Galoppini and R.A. Bartynski, J. Phys. Chem. C **118**, 12923 (2014).

27) “Measurement of the background in Auger-photoemission coincidence spectra (APECS) associated with inelastic or multi-electron valence, band photoemission process”, S. Satyal, P.V. Joglekar, K. Shastry, S. Kalaskar, Q. Dong, S.L. Hulbert, R.A. Bartynski and A.H. Weiss, J. Electron Spectrosc. Relat. Phenom. **195**, 66 (2014).

28) “Zinc(II) tetraphenylporphyrin adsorption on Au(111): an interplay between molecular self-assembly and surface stress”, C. Ruggieri, S. Rangan, R.A. Bartynski and E. Galoppini, J. Phys. Chem. C **119**, 6101 (2015).

29) “The solid state conversion reaction of epitaxial FeF_2(110) thin films with lithium studied by angle-resolved X-ray photoelectron spectroscopy”, R. Thorpe, S. Rangan, R.A. Bartynski, R. Whitcomb, A.C. Basaran, T. Saerbeck and I.K. Schuller, Phys. Chem. Chem. Phys. **17**, 15218 (2015).

30) “Investigation of SEI layer formation in conversion iron fluoride cathodes by combined STEM/EELS and XPS”, M. Sina, R. Thorpe, S. Rangan, N. Pereira, R.A. Bartynski, G.G. Amatucci and F. Cosandey, J. Phys. Chem. C **119**, 9762 (2015).

31) “Symmetry breaking charge transfer in a Zinc chlorodipyrrin acceptor for high open circuit voltage organic photovoltaics”, A.N. Bartynski, M. Gruber, S. Rangan, S. Mollinger, C. Trinh, S. Das, E. Couderc, S.E. Bradforth, K. Vandewal, A. Salleo, R.A. Bartynski, W. Brutting and M.E. Thompson, J. Am. Chem. Soc. **137**, 5397 (2015).

32) “Synthesis of zinc tetraphenylporphyrin rigid rods with a built-in dipole”, K. Chitre, A. Batarseh, A. Kopecky, H. Fan, H. Fang, R. Lalancette, R.A. Bartynski and E. Galoppini, J. Phys. Chem. B, **119**, 7522 (2015).

33) “Chemical interaction, space-charge layer and molecular charging energy for a TiO_2/TCNQ interface”, J. I. Martinez, F. Flores, J. Ortega, S. Rangan, C. Ruggieri and R.A. Bartynski, J. Phys. Chem. C, **119**, 22086 (2015)

34) “Photoelectrochemical properties of porphyrin dyes with a molecular dipole in the linker”, K.T. Ngo, J. Rochford, H. Fan, A. Batarseh, K. Chitre, S. Rangan, R.A. Bartynski and E. Galoppini, Faraday Discussions (2015), in press.

I. 5. Personnel and Collaborators

Dr. Wenhua Chen
Dr. Quantong Shen
Dr. Hao Wang
Grant Junno (physics undergraduate student)
Ryan Thorpe (physics graduate student)

Collaborators:
Prof. Jingguang G. Chen, Columbia University, NY
Prof. Timo Jacob, Ulm University, Germany
Dr. Payam Kaghazchi, Free University, Germany
Prof. Bruce E. Koel, Princeton University, PA
Prof. Torgny Gustafsson, Rutgers University, NJ
Prof. Leonard C. Feldman, Rutgers University, NJ

In the past, we have been working with Prof. Jingguang G. Chen from Columbia University (formerly University of Delaware) on the use of HREELS to characterize surface chemistry of NO on clean and oxygen-covered planar and faceted Ir(210) as well as NH_3 on clean planar and faceted Ir(210), with Prof. Timo Jacob from Ulm University and Dr. Payam Kaghazchi from Free University on the DFT calculations of geometries and energetics of adsorbate (O, C, N) on Ir and Re surfaces of substrate and facets as well as corresponding surface phase diagrams, with Prof. Bruce E. Koel from Princeton University (formerly Lehigh University) on the use of LEIS to characterize surface composition on metal (Au, Pt)-covered planar and faceted Re surfaces as well as Pt monolayer supported on faceted C/Re$(11\bar{2}1)$ surface, and with Prof. Torgny Gustafsson and Prof. Leonard C. Feldman from Rutgers University on the use of HIM to characterize real time surface morphology of faceted Au/C/Re$(12\bar{3}1)$ at atmospheric conditions.

I. 6. Presentations and Recognition for PI and Group Members

R.A. Bartynski and W. Chen were invited to write an invited review paper (a chapter) for a book entitled “Catalysis by Materials with Well-defined Structures” published by Elsevier BV in 2015 (ISBN: 978-0-12-801217-8).

R.A. Bartynski was named Fellow of the AAAS in December of 2014.

Chaz Ruggieri, winner of the Best Poster Competition, Physical Electronics Conference, June 2015.

R.A. Bartynski, invited talk, Low Energy Electrons: Dynamics and Correlation near Surfaces and Nanostructures Workshop, Castle Hemstein, Vienna, Austria, September 2015

R.A. Bartynski, five invited lectures, Graduate Course in Experimental Methods for the Determination of Structure and the Electronic Properties of Aggregated Systems with Low Dimensionality, Universita di Roma Tre, Rome, Italy, June 2015.

R.A. Bartynski, two invited lectures, 6th School of Nanostructures, U. Federico Santa Maria, Valparaiso, Chile, December 2013.

R. A. Bartynski, invited talk, Fun COS Opening Symposium, U. Erlangen-Nuremberg, Germany, Nov. 2013.

R. A. Bartynski, invited talk, DOE Solar Photochemistry Workshop, Annapolis, MD, June 2013.

R. A. Bartynski, invited talk, Chemistry Colloquium, U. Padova, Padova, Italy, April 2013.

R. A. Bartynski, invited 5 lectures, Graduate Course in Experimental Methods for the Determination of Structure and the Electronic Properties of Aggregated Systems with Low Dimensionality, Universita di Roma Tre, Rome, Italy, April/May 2013.

R. A. Bartynski, invited talk, Adamson Award Symposium, American Chemical Society, Spring Meeting, New Orleans, April 2013.

R. A. Bartynski, invited Condensed Matter Seminar, Universita di Roma Tre, Rome, Italy, Oct. 2012.

R. A. Bartynski was invited to give Condensed Matter Seminar, U. Roma II “Tor Vergatta”, Rome, Italy, Sept. 2012.

R. A. Bartynski, invited talk, Magnetic Order in Nanostructures and Spectroscopy Workshop, Rome, Italy, September 2012.

R. A. Bartynski, invited talk, DOE Solar Photochemistry Workshop, Annapolis, MD, June 2012.

R. A. Bartynski, invited Physical Chemistry Seminar, University of California - Riverside, Riverside, CA, June 2012.

R. A. Bartynski, invited Physics Colloquium, University of South Florida, Tampa, FL, Oct. 2011.

R. A. Bartynski, invited Physics Colloquium, University of North Carolina, Chapel Hill, NC, Oct. 2011.

R. A. Bartynski, invited talk, DOE Catalysis Workshop, Annapolis, MD, October 2011.

R. A. Bartynski, Chair, Department of Physics and Astronomy, Rutgers University, 2013-present.

R. A. Bartynski, DOE Review Committee, The Molecular Foundry, 2013

R. A. Bartynski, NSF Review Panel, DMREF program, 2013

R. A. Bartynski, Executive Committee, Surface Science Division of the American Vacuum Society, 2012-2015.

R. A. Bartynski, Director, Laboratory for Surface Modification, Rutgers University, 2007-2013.

W. Chen, poster presentation, Spring Symposium of the Catalysis Society of Metropolitan New York, Bethlehem, PA, March 12, 2014.

W. Chen, oral presentation, 245th American Chemical Society National Meeting, New Orleans, LA, April 7-10, 2013.

W. Chen, poster presentation, Spring Symposium of the Catalysis Society of Metropolitan New York, Princeton, NJ, March 20, 2013.

W. Chen, poster presentation, 244th American Chemical Society National Meeting, Philadelphia, PA, August 19-23, 2012.

W. Chen, poster presentation, Spring Symposium of the Catalysis Society of Metropolitan New York, Clinton, NJ, March 14, 2012.

W. Chen, poster presentation, 71st Physical Electronics Conference, Albany, NY, June 14-17, 2011.

W. Chen, poster presentation, Spring Symposium of the Catalysis Society of Metropolitan New York, Piscataway, NJ, March 16, 2011.

H. Wang, poster presentation, 75th Physical Electronics Conference, New Brunswick, NJ, June 17-19, 2015.

H. Wang, oral presentation, American Physical Society March Meeting, Denver, CO, March 3-7, 2014.

H. Wang, poster presentation, Spring Symposium of the Catalysis Society of Metropolitan New York, Bethlehem, PA, March 12, 2014.

Q. Shen, poster presentation, 244th American Chemical Society National Meeting, Philadelphia, PA, August 19-23, 2012.

Q. Shen, oral presentation, 58th American Vacuum Society International Symposium, Nashville, TN, Oct. 30 - Nov. 4, 2011.

Q. Shen, poster presentation, Spring Symposium of the Catalysis Society of Metropolitan New York, Piscataway, NJ, March 16, 2011.

I. 7. Funds

There will be no unexpected funds at the end of this grant period.

Bibliography and References Cited

1. T. E. Madey, J. Guan, C.-Z. Dong, S. M. Shivaprasad. "Morphological instabilities induced by ultrathin films on W(111)". *Surf. Sci.* **1993**, 287-288, 826.
2. T. E. Madey, J. Guan, C.-H. Nien, C.-Z. Dong, H.-S. Tao, R. A. Campbell. "Faceting induced by ultrathin metal films on W(111) and Mo(111): structure, reactivity, and electronic properties". *Surf. Rev. Lett.* **1996**, 3, 1315.

3. T. E. Madey, C. H. Nien, K. Pelhos, J. J. Kolodziej, I. M. Abdelrehim, H. S. Tao. "Faceting induced by ultrathin metal films: structure, electronic properties and reactivity". *Surf. Sci.* **1999**, 438, 191.

4. T. E. Madey, K. Pelhos, Q. Wu, R. Barnes, I. Ermanoski, W. Chen, J. J. Kolodziej, J. E. Rowe. "Nanoscale surface chemistry". *Proc. Natl. Acad. Sci. U.S.A.* **2002**, 99, 6503.

5. T. E. Madey, W. Chen, H. Wang, P. Kaghazchi, T. Jacob. "Nanoscale surface chemistry over faceted substrates: structure, reactivity and nanotemplates". *Chem. Soc. Rev.* **2008**, 37, 2310.

6. H. Wang, W. Chen, R. A. Bartynski. "Oxygen-induced nano-faceting of Re(11-21)". *Surf. Sci.* **2015**, 635, 85.

7. P. L. Hansen, J. B. Wagner, S. Helveg, J. R. Rostrup-Nielsen, B. S. Clausen, H. Topsøe. "Atom-Resolved Imaging of Dynamic Shape Changes in Supported Copper Nanocrystals". *Science* **2002**, 295, 2053.

8. M. A. Newton, C. Belver-Coldeira, A. Martínez-Arias, M. Fernández-García. "Dynamic in situ observation of rapid size and shape change of supported Pd nanoparticles during CO/NO cycling". *Nat. Mater.* **2007**, 6, 528

9. P. Nolte, A. Stierle, N. Y. Jin-Phillipp, N. Kasper, T. U. Schulli, H. Dosch. "Shape Changes of Supported Rh Nanoparticles During Oxidation and Reduction Cycles". *Science* **2008**, 321, 1654.

10. X. Yang, B. E. Koel, H. Wang, W. Chen*, R. A. Bartynski. "Nanofaceted C/Re(11-21): Fabrication, Structure, and Template for Synthesizing Nanostructured Model Pt Electrocatalyst for Hydrogen Evolution Reaction". *ACS Nano* **2012**, 6, 1404.

11. F. Atamny, A. Baiker. "Investigation of carbon-based catalysts by scanning tunneling microscopy: Opportunities and limitations". *Appl. Catal. A* **1998**, 173, 201.

12. E. Nikolla, A. Holewinski, J. Schwank, S. Linic. "Controlling Carbon Surface Chemistry by Alloying: Carbon Tolerant Reforming Catalyst". *J. Am. Chem. Soc.* **2006**, 128, 11354.

13. C. J. Weststrate, A. C. Kızılkaya, E. T. R. Rossen, M. W. G. M. Verhoeven, I. M. Ciobîcă, A. M. Saib, J. W. Niemantsverdriet. "Atomic and Polymeric Carbon on Co(0001): Surface Reconstruction, Graphene Formation, and Catalyst Poisoning". *J. Phys. Chem. C* **2012**, 116, 11575.

14. R. H. Baughman, A. A. Zakhidov, W. A. d. Heer. "Carbon Nanotubes--the Route Toward Applications". *Science* **2002**, 297, 787.

15. A. K. Geim. "Graphene: Status and Prospects". *Science* **2009**, 324, 1530.

16. K. F. Tan, J. Xu, J. Chang, A. Borgna, M. Saeys. "Carbon deposition on Co catalysts during Fischer–Tropsch synthesis: A computational and experimental study". *J. Catal.* **2010**, 274, 121.

17. P. Kaghazchi, T. Jacob, X. Yang, G. Junno, H. Wang, W. Chen, B. E. Koel, R. A. Bartynski. "Theoretical Study of Carbon Adsorption on Re Surfaces: Morphological Instability". *Catal. Lett.* **2014**, 144, 1667.

18. P. Kaghazchi, T. Jacob, I. Ermanoski, W. Chen, T. E. Madey. "First-Principles Studies on Oxygen-Induced Faceting of Ir(210)". *ACS Nano* **2008**, 2, 1280.

19. H. Wang, W. Chen, R. A. Bartynski, P. Kaghazchi, T. Jacob. "Nitrogen-induced reconstruction and faceting of Re(11-21)". *J. Chem. Phys.* **2014**, 140, 024707.

20. M. Asscher, J. Carrazza, M. M. Khan, K. B. Lewis, G. A. Somorjai. "The ammonia synthesis over rhenium single-crystal catalysts: Kinetics, structure sensitivity, and effect of potassium and oxygen". *J. Catal.* **1986**, 98, 277.

21. G. A. Somorjai, N. Materer. "Surface structures in ammonia synthesis". *Top. Catal.* **1994**, 1, 215.

22. K. Honkala, A. Hellman, I. N. Remediakis, A. Logadottir, A. Carlsson, S. Dahl, C. H. Christensen, J. K. Nørskov. "Ammonia Synthesis from First-Principles Calculations". *Science* **2005**, 307, 555.

23. H. Wang, Q. Shen, W. Chen, R. A. Bartynski. "Carbon-induced faceting of Re(12-31)". **in preparation**.

24. Q. Shen, W. Chen, H. Wang, R. A. Bartynski. "Morphological stability of oxygen- and nitrogen-covered Ru(11-21)". *J. Chem. Phys.* **2013**, 139, 084707.

25. Q. Shen, W. Chen, H. Wang, Govind, T. E. Madey, R. A. Bartynski. "Nano-faceting of the Ru(11-20) surface". *Surf. Sci.* **2010**, 604, L12.

26. Q. Shen, H. Wang, W. Chen, R. A. Bartynski. "Branching in oxygen-induced faceting of Ru(11-21)". **in preparation**.

27. H. Dietrich, P. Geng, K. Jacobi, G. Ertl. "Sticking coefficient for dissociative adsorption of N_2 on Ru single crystal surfaces ". *J. Chem. Phys.* **1996**, 104, 375.

28. H. Dietrich, K. Jacobi, G. Ertl. "Decomposition of NH_3 on Ru(11-21)". *Surf. Sci.* **1996**, 352-354, 138.

29. I. Ermanoski, K. Pelhos, W. Chen, J. S. Quinton, T. E. Madey. "Oxygen-induced nano-faceting of Ir(210)". *Surf. Sci.* **2004**, 549, 1.

30. W. Chen, I. Ermanoski, T. E. Madey. "Decomposition of Ammonia and Hydrogen on Ir Surfaces: Structure Sensitivity and Nanometer-Scale Size Effects". *J. Am. Chem. Soc.* **2005**, 127, 5014.

31. W. Chen, R. A. Bartynski, P. Kaghazchi, T. Jacob. "Oxidation of CO by NO on planar and faceted Ir(210)". *J. Chem. Phys.* **2012**, 136, 224701.

32. W. Chen, T. E. Madey, A. L. Stottlemyer, J. G. Chen, P. Kaghazchi, T. Jacob. "Structure Sensitivity in Adsorption and Decomposition of NO on Ir". *J. Phys. Chem. C* **2008**, 112, 19113.

33. W. Chen, A. L. Stottlemyer, J. G. Chen, P. Kaghazchi, T. Jacob, T. E. Madey, R. A. Bartynski. "Adsorption and decomposition of NO on O-covered planar and faceted Ir(210)". *Surf. Sci.* **2009**, 603, 3136.

34. W. Chen, Q. Shen, R. A. Bartynski, P. Kaghazchi, T. Jacob. "Reduction of NO by CO on Unsupported Ir: Bridging the Materials Gap". *ChemPhysChem* **2010**, 11, 2515.

35. W. Chen, I. Ermanoski, T. Jacob, T. E. Madey. "Structure Sensitivity in the Oxidation of CO on Ir Surfaces". *Langmuir* **2006**, 22, 3166.

36. P. Kaghazchi, T. Jacob, W. Chen, R. A. Bartynski. "Theoretical and experimental studies of hydrogen adsorption and desorption on Ir surfaces ". *Phys. Chem. Chem. Phys.* **2013**, 15, 12815.

37. W. Chen, Q. Shen, R. A. Bartynski, P. Kaghazchi, T. Jacob. "Reduction of Nitric Oxide by Acetylene on Ir Surfaces with Different Morphologies: Comparison with Reduction of NO by CO". *Langmuir* **2013**, 29, 1113.

38. W. Chen, I. Ermanoski, Q. Wu, T. E. Madey, H. H. Hwu, J. G. Chen. "Adsorption and decomposition of acetylene on planar and faceted Ir(210)". *J. Phys. Chem. B* **2003**, 107, 5231.

39. W. Chen, Q. Shen, R. A. Bartynski. "Selective Oxidation of Ammonia by Co-adsorbed Oxygen on Iridium Surfaces: Formation of N_2O". *Catal. Lett.* **2015**, 145, 757.

40. J. L. Gland, V. N. Korchak. "Ammonia oxidation on a stepped platinum single-crystal surface". *J. Catal.* **1978**, 53, 9.

41. A. C. M. van den Broek, J. van Grondelle, R. A. van Santen. "Determination of Surface Coverage of Catalysts: Temperature Programmed Experiments on Platinum and Iridium Sponge Catalysts after Low Temperature Ammonia Oxidation". *J. Catal.* **1999**, 185, 297.

42. M. Baerns, R. Imbihl, V. A. Kondratenko, R. Kraehnert, W. K. Offermans, R. A. v. Santen, A. Scheibe. "Bridging the pressure and material gap in the catalytic ammonia oxidation: structural and catalytic properties of different platinum catalysts". *J. Catal.* **2005**, 232, 226.

43. J. Gong, R. A. Ojifinni, T. S. Kim, J. M. White, C. B. Mullins. "Selective Catalytic Oxidation of Ammonia to Nitrogen on Atomic Oxygen Precovered Au(111)". *J. Am. Chem. Soc.* **2006**, 128, 9012.

44. N. López, M. García-Mota, J. Gómez-Díaz. "NH_3 Oxidation on Oxygen-Precovered Au(111): A Density Functional Theory Study on Selectivity". *J. Phys. Chem. C* **2008**, 112, 247.

45. J. Gong, C. B. Mullins. "Surface Science Investigations of Oxidative Chemistry on Gold". *Acc. Chem. Res.* **2009**, 42, 1063.

46. L. Chmielarz, M. Jabłońska, A. Strumiński, Z. Piwowarska, A. Węgrzyn, S. Witkowski, M. Michalik. "Selective catalytic oxidation of ammonia to nitrogen over Mg-Al, Cu-Mg-Al and Fe-Mg-Al mixed metal oxides doped with noble metals". *Appl. Catal. B* **2013**, 130-131, 152.

47. Q. Shen, W. Chen, R. A. Bartynski. "Growth of gold nanoparticles on faceted O/Ru(11–20) nanotemplate". *Surf. Sci.* **2011**, 605, 1457.

48. M. Reyhan, H. Wang, T. E. Madey. "Preferential Nucleation of Metallic Clusters on a Nanotemplate: Co on Oxygen-Faceted Re(12-31) ". *Catal. Lett.* **2009**, 129, 46.

49. J. Greeley, T. F. Jaramillo, J. Bonde, I. B. Chorkendorff, J. K. Norskov. "Computational high-throughput screening of electrocatalytic materials for hydrogen evolution". *Nat. Mater.* **2006**, 5, 909.

50. J. Greeley, J. K. Nørskov, L. A. Kibler, A. M. El-Aziz, D. M. Kolb. "Hydrogen Evolution Over Bimetallic Systems: Understanding the Trends". *ChemPhysChem* **2006**, 7, 1032.

51. T. F. Jaramillo, K. P. Jørgensen, J. Bonde, J. H. Nielsen, S. Horch, I. Chorkendorff. "Identification of Active Edge Sites for Electrochemical H_2 Evolution from MoS_2 Nanocatalysts ". *Science* **2007**, 317, 100.

52. D. V. Esposito, S. T. Hunt, A. L. Stottlemyer, K. D. Dobson, B. E. McCandless, R. W. Birkmire, J. G. Chen. "Low-Cost Hydrogen-Evolution Catalysts Based on Monolayer Platinum on Tungsten Monocarbide Substrates". *Angew. Chem. Int. Ed.* **2010**, 49, 9859.

53. M. E. Björketun, A. S. Bondarenko, B. L. Abrams, I. Chorkendorff, J. Rossmeisl. "Screening of electrocatalytic materials for hydrogen evolution". *Phys. Chem. Chem. Phys.* **2010**, 12, 10536.

54. Y. Li, H. Wang, L. Xie, Y. Liang, G. Hong, H. Dai. "MoS2 Nanoparticles Grown on Graphene: An Advanced Catalyst for the Hydrogen Evolution Reaction". *J. Am. Chem. Soc.* **2011**, 133, 7296.